International Journal of Nanoelectronics and Materials
IJNeaM
ISSN 1985-5761 | E-ISSN 2232-1535

Properties of porous gallium nitride under varying etching durations of low temperature photoelectrochemical etching

Hannes Zuleikha Zaidi [a], Rosfariza Radzali [a] *, Ainorkhilah Mahmood [b], Anis Nabilah Mohd Daud [a], Alhan Farhanah Abd Rahim [a], Nor Shahanim Mohamad Hadis [a], Mohd Hanapiah Abdullah [a], and Aslina Abu Bakar [a]

[a]*Electrical Engineering Studies, Universiti Teknologi MARA Cawangan Pulau Pinang, Permatang Pauh Campus, 13500 Permatang Pauh, Pulau Pinang, Malaysia*
[b]*Department of Applied Sciences, Universiti Teknologi MARA Cawangan Pulau Pinang, Permatang Pauh Campus, 13500 Permatang Pauh, Pulau Pinang, Malaysia*
∗ Corresponding author. Tel.: +017-5830840; e-mail: rosfariza074@uitm.edu.my

Received 18 August 2024, Revised 18 October 2024, Accepted 05 November 2024

ABSTRACT

In this work, porous gallium nitride (PGaN) samples were fabricated via photoelectrochemical etching (PEC) under low temperature (LT) conditions. The effect of etching duration during the low temperature photoelectrochemical etching (LT-PEC) on the structural and morphological properties of PGaN structures was investigated. A continuous current density of 60 mA/cm^2 and potassium hydroxide (KOH) electrolyte were used during the etching process at different etching durations of 40, 60, and 90 minutes. Field emission scanning electron microscopy (FESEM) revealed that PGaN etched for 60 minutes exhibited the smallest pore diameter (27.23 nm) and highest estimated porosity (36.0%). Its pore diameter and the estimated average pore depth also increased as the duration increased. Furthermore, atomic force microscopy (AFM) revealed that the root mean square (RMS) surface roughness increased as the etching duration increased. The Raman spectra of the E_2(high) phonon mode of all the PGaN samples had shifted to a lower frequency than that of the as-grown GaN due to the stress relaxation. Lastly, the intensities of the Raman spectra of the PGaN samples increased as the duration increased, indicating more efficient light scattering in their porous structures. Therefore, the enhanced PGaN properties indicate that they possess good potential for implementation in sensing device applications.

Keywords: *Etching duration, Photoelectrochemical etching, Low temperature, Porous GaN*

1. INTRODUCTION

Porous III-nitrides such as porous gallium nitride (PGaN) have been widely researched due to their better properties relative to as-grown GaN because porous structure could provide a high surface area to volume ratio, shift of band gap, and enhanced luminescence intensity [1]. A few techniques can be used in the etching process to create PGaN; namely, wet and dry etching. Dry etching is the process of removing materials by subjecting them to an ion bombardment, such as chlorine or oxygen while wet etching is a wafer material removal technique that employs liquid chemicals or etchants as the main remover. The dry etching technique, however, may cause surface damage on the material as mentioned in [2, 3], and the process is costly. Apart from dry etching, wet etching such as photoelectrochemical (PEC) etching which is more cost-effective and convenient has also been used to create porous structures on GaN and has been the subject of numerous studies including research done in [2, 4–6]. The PEC etching technique provides minimal structural damage, simplicity, and low processing costs [7, 8]. In addition to that, the use of ultraviolet (UV) light during PEC further aids pore formation on GaNs' surface. Upon the UV illumination on the GaN surface, electrons will be excited to the conduction band and holes are generated at the valence band which subsequently participate in the oxidation and dissolution of the substrate [9]. Previous research has also looked into the differences between producing porous III-nitrides using different light sources [10]. According to the findings, porous structures exposed to UV created higher pore density and deeper voids than those not illuminated by UV light.

However, UV illumination during PEC produces heat. This heat will vaporize the electrolyte and reduce the volume of electrolyte used to fabricate PGaN. Based on the research done by Balagurov et. al [11], the composition of electrolytes was seen to have changed due to the partial evaporation of electrolytes at elevated temperatures that caused a decrease in critical current density which affects the etching process. Furthermore, investigation on PGaN at different etching durations using the electrochemical etching method has been conducted previously [4, 12]. It was reported that as the etching duration increased, the diameter of the porous structure increased. However, these experiments conducted by [4] were carried out at room temperature. It was found that porous structures etched at room temperature produced non-uniform porous distribution with larger diameter porous [2, 4].

Despite some research being done on the impact of

temperature on the quality of porous silicon such as in [13], to our best knowledge, the fabrication of PGaN using direct-current low-temperature photoelectrochemical etching (LT-PEC) is still at an early stage and many fundamentals' properties has not yet been explored. Thus, in this work, PGaN was fabricated at low-temperature conditions to overcome the problem caused by the heat from the UV illumination. The effect of etching duration on the PGaN optical and structural features was examined using a field emission scanning electron microscope (FESEM), high-resolution X-ray diffractometer (HR-XRD), atomic force microscope (AFM), and Raman spectroscopy.

2. METHODOLOGY

The present study used commercially available n-type GaN wafers that were unintentionally doped and grown on sapphire substrates measuring 2 inches in diameter. The wafer was then cleaved into several 1 cm × 1 cm pieces. Prior to PEC, a solution containing a 1:20 ratio of ammonium hydroxide (NH_4OH) dissolved in water (H_2O) was used to remove the oxide present on GaN. This was followed by a solution with a 1:50 ratio of hydrofluoric acid dissolved in H_2O. Finally, the pieces were cleaned by boiling in an aqua regia solution containing a 3:1 ratio of hydrochloric acid (HCl) and nitric acid (HNO_3).

Next, PGaN was fabricated by utilizing the proposed LT-PEC. A water-cooling circulation system was employed to maintain the LT-PEC at a stable temperature between 10 and 15°C throughout the etching process. The LT-PEC was conducted in a Teflon anodization cell with a central circular hole. The GaN sample was placed horizontally at the bottom of the cell, pressed against the O-ring by a metal plate, and fixed as the anode, while a platinum (Pt) wire served as the cathode. The GaN sample was etched with a 4% concentration of potassium hydroxide (KOH) electrolyte under 100W UV light for 45, 60, and 90 minutes, with a constant current density of 60 mA/cm^2. Following the LT-PEC process, the morphological characteristics of PGaN samples were analyzed using field emission scanning electron microscopy (FESEM, Model: XHR-FESEM FEI Verios 460L) and atomic force microscopy (AFM, Model: Dimension EDGE, BRUKER). Energy-dispersive X-ray spectroscopy (EDX) was also performed to ascertain the material composition of the PGaN surface.

NanoScope analysis was deployed for conducting AFM analysis to explore the surface roughness and estimate the average pore depth. High-resolution X-ray diffraction (HR-XRD, Model: PANalytical X'Pert Pro MRD PW3040) was utilized to assess the crystalline properties of the samples. The optical properties of PGaN were examined via Raman spectroscopy, conducted using a Renishaw inVia Raman microscope system with a 20 mW HeNe laser (λ=633 nm) in z(x, unpolarized)$\bar{z}$ scattering configuration.

3. RESULTS AND DISCUSSION

Photoelectrochemical etching (PEC) is a process in which the semiconductor surface is initially oxidized, followed by the dissolution of the resultant oxides. A redox reaction occurs when GaN comes into contact with the KOH electrolyte, resulting in the formation of PGaN. Upon UV-light illumination, electrons obtain enough energy to be excited to a higher energy level, allowing them to exist in the conduction band. Simultaneously, holes are generated in the valence band as electrons are excited.

An upward band bending occurs on GaN films' surfaces when they come into contact with the KOH electrolyte. Upward band bending pushes electrons away from the interface and pulls holes closer to it. When electrons reach the platinum (Pt) electrode, they engage in a cathodic reaction with water molecules in the electrolyte, producing hydrogen gas. As the holes are drawn to the GaN/KOH interface, the surface of GaN becomes more oxidized and increases the oxidation state of the surface. Furthermore, holes are further collected at the GaN surface upon UV illumination and enhance the flow of electrons toward the Pt electrode. This process increases electron depletion at the GaN's surface, which results in a further increment in the oxidation state of the GaN's surface [14]. The decomposition of GaN is assumed to result in the formation of GaN^{3+} with the development of nitrogen gas [15] as shown in Equation (1):

$$2GaN_{(s)} + 6h^+ \longrightarrow 2Ga^{3+} + N_2 \quad (1)$$

Meanwhile, an oxidation reaction occurs between the positively charged Ga^{3+} ions and the OH^- ions from the electrolyte, forming Ga-based hydroxides, specifically $Ga(OH)_3$ as shown in Equation (2):

$$Ga^{3+} + 3OH^- \longrightarrow Ga(OH)_3 \quad (2)$$

Furthermore, the following OH^- reaction on the hydroxides leads to the formation of hydroxides that are soluble in water, as shown Equation (3). Subsequently, the disintegration process results in the creation of porous GaN formations.

$$Ga(OH)_3 + OH^- \longrightarrow Ga_2(OH)_4^- \quad (3)$$

The surface morphologies of the PGaN samples etched for 45, 60, and 90 minutes were examined using FESEM (Figure 1). As shown in Figure 1a, the as-grown GaN exhibited a smooth and flat surface without any pores prior to LT-PEC treatment. However, after 45 minutes of LT-PEC, hexagonal-like structures with an average diameter of 221.76 nm began to form on the PGaN's surface (Figure 1b). At this initial stage of the LT-PEC process, these hexagonal-like structures were shallow, with pores observed in only a few areas. A similar hexagonal pore pattern in PGaN structures has been observed in previous studies [16].

For the PGaN sample etched for 60 minutes, a significant change in its surface morphology was observed (Figure 1c). The formation of PGaN structures was more pronounced, with a higher density of fairly uniform hexagonal pores compared to the 45-minute PGaN.

At this stage, etching primarily occurred at the center of the grain structures, leaving the grain boundaries unetched, thereby revealing the hexagonal porous structures. In addition to the higher pore density, the average pore diameter of the 60-minute PGaN was 27.23 nm, which is smaller than that of the 45-minute sample. Furthermore, the pore diameters of the 60-minute PGaN were smaller than those reported by other research groups, which were obtained using PEC at room temperature conditions [12, 17].

The result demonstrates that LT-PEC significantly impacts the surface morphology and the formation of PGaN structures. Lowering the temperature during PEC not only increased the pore density but also resulted in more uniform and smaller pore diameters. Moreover, the discrepancy in pore sizes between our study and those of [12, 17] further supports the idea that pore diameters of PGaN samples decrease during LT-PEC. The high density, uniformity, and small pore size of the etched PGaN can be attributed to the low etching temperature, which may enhance the current efficiency of the dissolution process, and result in increased porosity of the porous PGaN structure [13]. Similar results were observed in [13] where a greater number of pores with smaller diameters were achieved by lowering the etching temperature. In addition, [11] reported a more uniform pore as the etching temperature decreased.

As the etching duration increased to 90 minutes, pore formation in the PGaN became more obvious. As shown in Figure 1d, the structure underwent a significant change compared to the 45- and 60-minute PGaN samples.

At this stage, larger hexagonal pores were produced as the smaller pores merged with their surrounding pores. In addition to that, dissolution at the center of the grain became more prominent, leading to an increase in pore size. The average pore diameter of the 90-min PGaN was measured to be 119.53 nm. This study determined that as the etching duration increased the pore size grew larger.

ImageJ software was used to estimate the porosity of the PGaN samples. The detailed methodology for porosity calculation has been explained in our previous work [18]. A similar approach for calculating the porosity of porous structures has also been carried out by other researchers [19, 20]. Overall, it was observed that the porosity increased as the etching duration increased. The 45-minute PGaN exhibited the lowest estimated porosity (6.7%). This result may be due to insufficient etching time to produce pores on the GaN's surface. Meanwhile, the 60-minute PGaN sample showed the highest estimated porosity (36.0%) while the 90-minute PGaN sample had a porosity of 28.3%. These results show that the high density and porosity of the 60-minute PGaN make it a promising candidate for optical and sensing device applications.

AFM measurement was employed to ascertain the average surface roughness in root mean square (RMS) value. Figure 2 displays the 3D AFM images of as-grown GaN and PGaN samples etched for varying etching durations. The relationship between RMS surface roughness and estimated average pore depth with etching duration is illustrated in

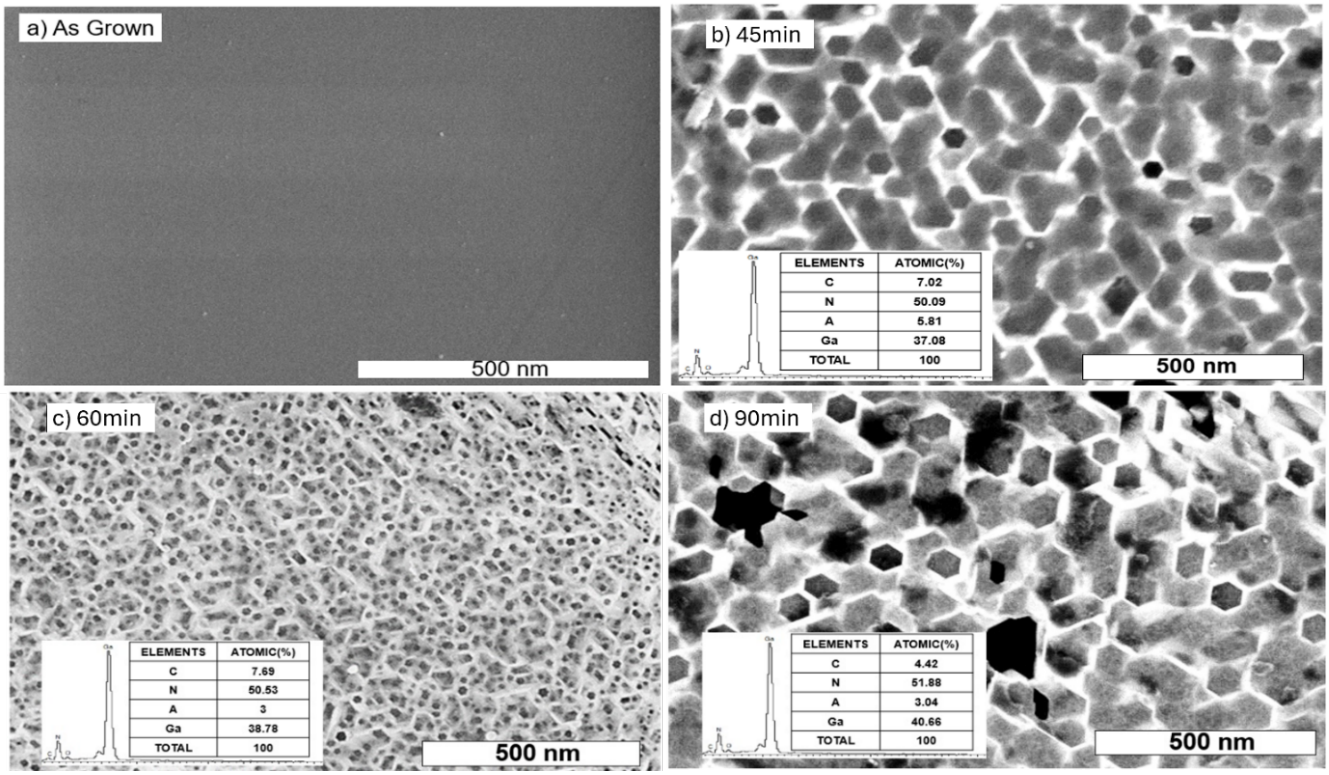

Figure 1. The FESEM images of as-grown GaN and PGaN samples were obtained at different LT-PEC durations: (a) as-grown, (b) 45 minutes, (c) 60 minutes, and (d) 90 minutes

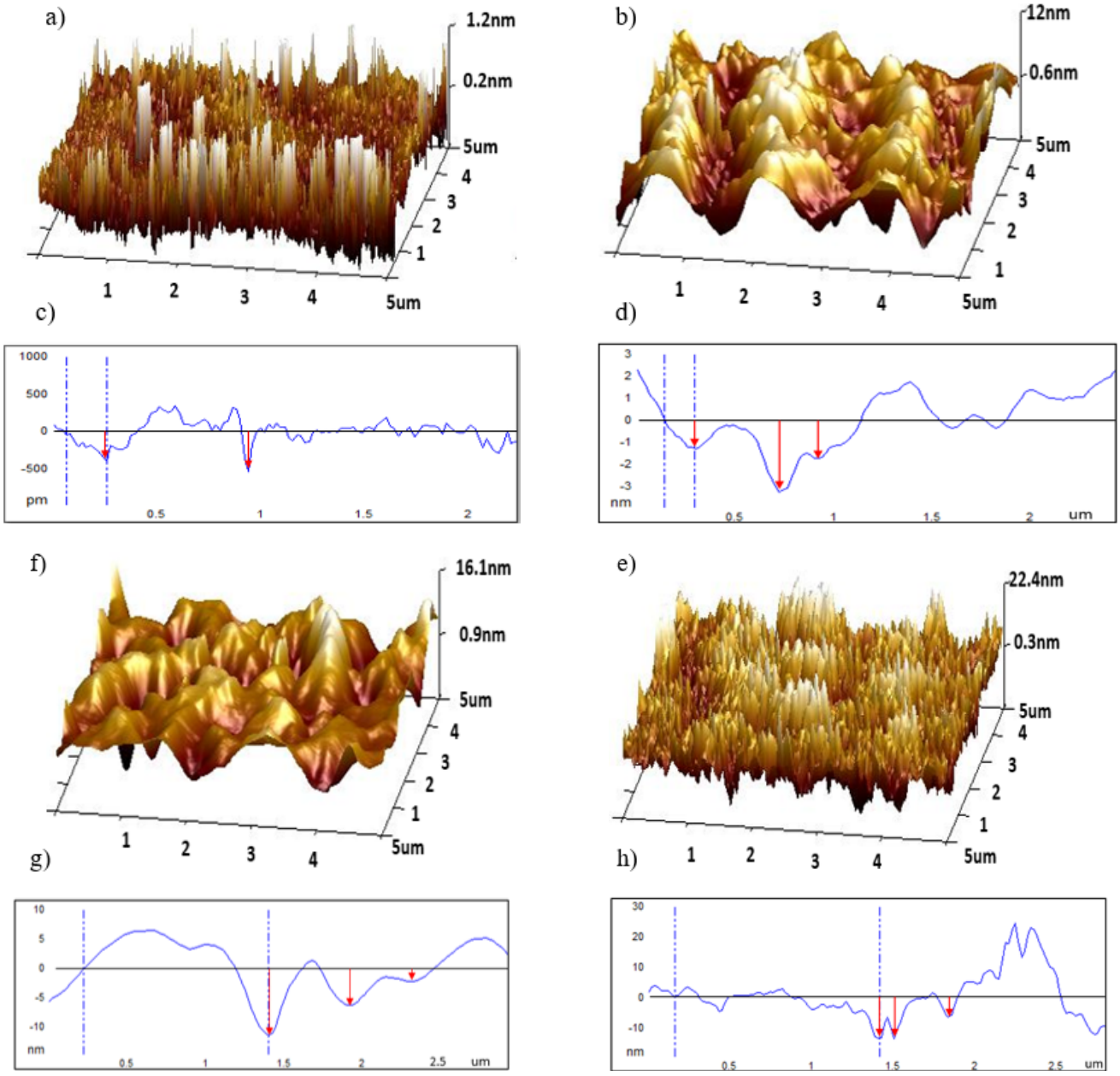

Figure 2. The AFM measurements of as-grown and PGaN were obtained at different LT-PEC durations; (a) as-grown GaN, (b) 45 minutes, (d) 60 minutes, (f) 90 minutes and line scan tool used to calculate the estimated average pore depth using NanoScope Analysis

Figure 3. To estimate the average pore depth, the cross-section line scan tool of NanoScope Analysis was used, which is a non-destructive method. Multiple crosslines were drawn on the AFM image, and the average pore depth was measured by the vertical distance between two cursors from the sample surface to the pore depth, as depicted in Figure 2(c, d, g, h). The average pore depth of the PGaN was estimated using a similar technique as in research conducted by [6, 21–24].

The as-grown sample as depicted in Figure 2(a), exhibits a smooth surface with a small RMS value of 0.57 nm. Because of the absence of pores on the as-grown GaN sample surfaces the estimated average pore depth value was not calculated for this sample. It is anticipated that as the etching duration rises, the surface roughness (RMS value) of the PGaN will also rise.

As indicated in Figure 3, all porous samples exhibited a greater RMS surface roughness in comparison to the as-grown sample. The reason behind this is that the photoelectrochemical etching (PEC), alters the surface morphology of the GaN film, thereby raising both the estimated average pore depth and surface roughness of the PGaN. For the 45-minute PGaN sample, the RMS surface roughness and estimated average pore depth value increased to 3.84 nm and 4.42 nm, respectively. The 60- and 90-minute PGaN samples showed a similar growth pattern. The 60-minute PGaN exhibited RMS surface roughness of 5.58 nm and an estimated pore depth of 5.63 nm. For the 90-minute PGaN sample, the RMS surface roughness increased slightly, peaking at 5.90 nm, with an estimated pore depth of 8.90 nm. The 60- and 90-minute PGaN samples exhibited a higher RMS surface roughness and estimated pore depth values than the 45-minute sample,

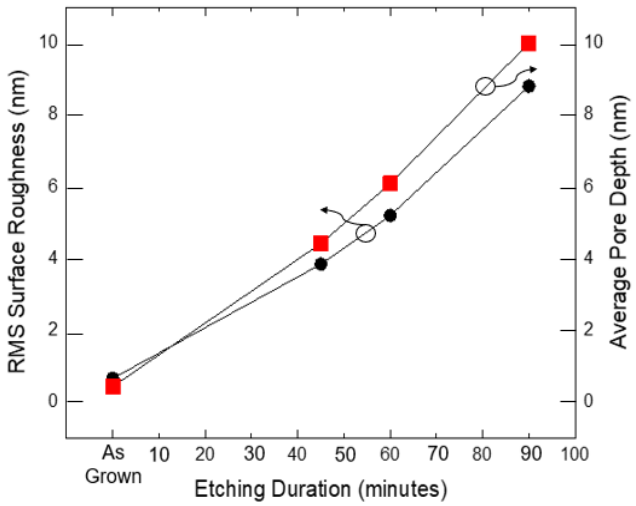

Figure 3. The RMS surface roughness and estimated average pore depth of PGaN samples at varying etching durations

indicating that etching duration significantly impacts surface roughness and pore depth. This is because, as the LT-PEC process progresses, the depth and density of the pores also grow, making the surface appear rougher [5]. From this outcome, it can also be inferred that longer etching durations resulted in deeper etching of the GaN samples, thereby increasing their RMS surface roughness and estimated average pore depth.

High-resolution X-ray diffraction (HR-XRD) was used to analyze the crystalline quality and lattice parameters of as-grown GaN and PGaN samples etched at different etching durations. Figure 4 displays the 2θ scan of HR-XRD data for all the samples while Table 1 summarizes the diffraction peak position, the full-width half maximum (FWHM), average crystallite size, and peak intensity of the PGaN samples that had undergone varying etching durations of LT-PEC. Diffraction peaks attributed to GaN (0002) and (0004) planes appeared at around 34.5° and 73.03°, respectively, while the peak at around 41.6° was attributed to the sapphire substrate.

From Table 1, the peak position of GaN (0002) in the 45- and 90-minute PGaN samples was consistent with that of the as-grown GaN, with a minimal peak shift. However, the peak position of the 60-minute PGaN sample at the (0002) plane exhibited a shift toward the lower angle, indicating an occurrence of stress in the PGaN samples [25].

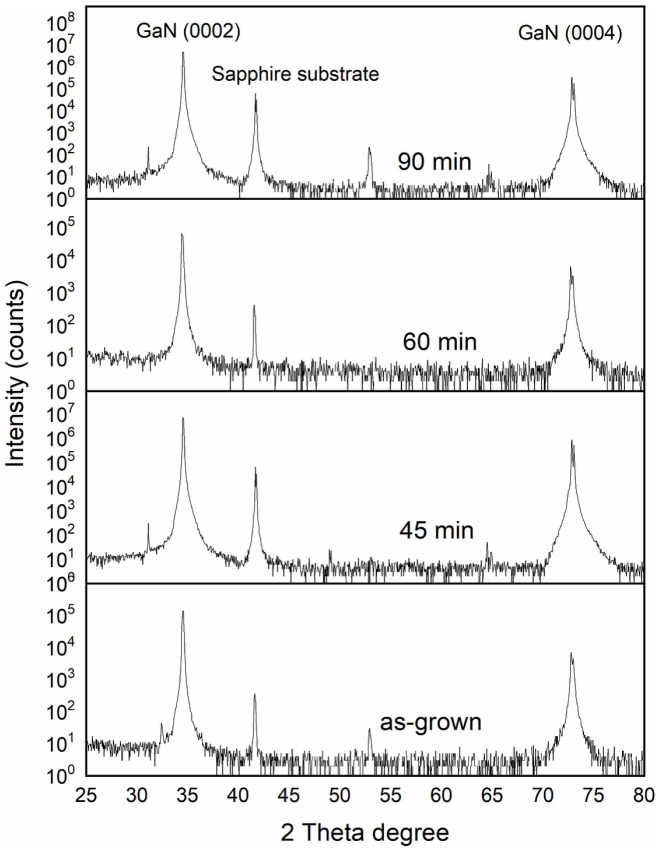

Figure 4. The 2θ scan data of as-grown and PGaN samples

Furthermore, the peak intensity of GaN (0002) for all PGaN samples was higher than that of the as-grown sample. Moreover, the ω-scan results of HR-XRD rocking curves (RC) of the asymmetric ($10\bar{1}2$) and symmetric (0002) planes were carried out to determine the as-grown GaN and PGaNs' edge plus mix and screw plus mix dislocation density, respectively. Overall, the FWHM value of the PGaNs was higher than that of the as-grown GaN. This could be due to the formation of non-stoichiometric Ga- or N-surfaces on the PGaN samples following the LT-PEC process [10, 25] which subsequently, increased their screw and edge plus mix dislocation densities. The HR-XRD results show that pore formation affects the peak intensities and positions as well as FWHM values of the PGaN samples.

Figure 5 depicts the Raman spectra of the as-grown GaN and PGaN samples. The internal stress of all samples was monitored by detecting the frequency and the characteristics of the polarization of the active phonons in

Table 1. A summary of the peak intensities and positions of the GaN (0002), average crystallite size, FWHM of RC (0002), and screw and edge plus mix dislocation densities of as-grown GaN and PGaN samples that have undergone various LT-PEC etching durations

Samples	Peak position GaN (0002) (°)	Peak intensity of GaN (0002) (count)	FWHM RC (0002) (arcmin)	FWHM RC ($10\bar{1}2$) (arcmin)	$N_{screw\ plus\ mix}$ dislocation density (cm^{-2})	$N_{edge\ plus\ mix}$ dislocation density (cm^{-2})
as-grown	34.555	14,715	3.510	6.23	8.91×10^{7}	7.43×10^{8}
45 minutes	34.582	6,898,823	3.696	6.50	9.88×10^{7}	8.09×10^{8}
60 minutes	34.477	61,644.47	3.642	6.57	9.59×10^{7}	8.27×10^{8}
90 minutes	34.582	4,711,248	3.720	6.67	1×10^{8}	8.52×10^{8}

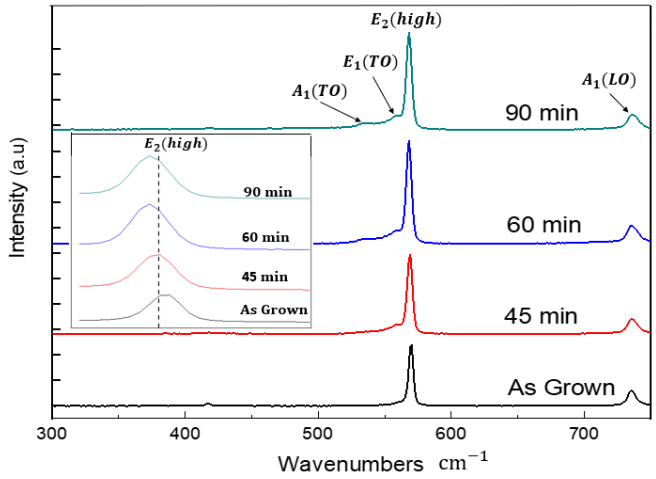

Figure 5. Raman spectra of the PGaN samples etched via LT-PEC at various etching durations

the Raman spectra. The stress relaxation that occurred in the PGaN samples was measured by determining the shift of the E_2(high) phonon line relative to that of the as-grown GaN. The E_2(high) phonon line of the 45-, 60-, and 90-minute PGaN samples shifted by 0.83, 1.70, and 1.79 cm^{-1}, respectively. Therefore, their corresponding compressive stress relaxations were 0.20±0.02, 0.40±0.02, and 0.42±0.02 GPa, respectively. The redshift of the E_2(high) phonon mode of PGaN samples increased with the duration of etching, which further confirmed the strain relaxation of the porous samples after porosification [26]. The amount of stress relaxation was determined using the equation: $\Delta W_{E2} = K_R \sigma$, where K_R is the proportionality (4.2 cm^{-1} GPa^{-1}) and 'σ' represents the in-plane biaxial stress. Moreover, under the Raman selection rules, A_1(LO) and E_2(high) are the only allowed phonon modes in the scattering geometry [14].

Furthermore, the spectra from the measurement are primarily characterized by E_2(high) and A_1(LO) phonons at approximately 569 and 734 cm^{-1}, respectively, aligning with wurtzite GaN Raman selection rules [27]. However, unlike as-grown GaN, all PGaNs exhibited A_1 transverse optical (TO) and E_1(TO) phonon modes. The presence of these two peaks points towards altered optical properties in the PGaN, likely due to crystal lattice disordering. This crystal lattice disordering may enhance the light scattering from the porous structure sidewalls [8, 28] and may eventually change the polarization of the light [29]. Additionally, the roughness and internal angles of such faceted crystallites influence light reflection and refraction through repeated scattering from a porous network built on randomly oriented GaN crystallites. The Raman intensities of all the samples are tabulated in Table 2. The Raman intensities of the PGaN samples were higher than that of the as-grown GaN. In addition to that, the etching duration has impacted the intensity augmentation and changed significantly as the surface morphology changed [25]. The Raman intensities increased as the etching duration increased, with the 60-minute PGaN sample exhibiting the highest Raman intensity. This enhancement can be attributed to the high density of small pores and the increased of porosity this sample compared to other porous samples. Thus, eventually improving the optical behaviour of the material. This observation is also supported by [25], which reported that a higher proportion of pores area resulted in greater porosity, thereby leading to a higher Raman intensity. It was found that multiple light scatterings were affected by the different surface roughness and internal angles of such faceted crystallites [25]. Furthermore, the increased anti-reflectivity resulting from surface roughening and the porous structure, which has a larger surface area, also contributed to these effects [30].

Furthermore, the Raman intensities of the PGaN samples increased with longer etching durations, indicating more efficient light scattering in their porous structures [26]. PGaN has a greater specific surface area, which increases its Raman intensities better than that of the as-grown GaN, allowing it to function as a light trap and reduce reflectance [31, 32]. The increase in the Raman intensity with longer etching durations as shown in Table 2, can be attributed to the greater number of photons scattered by the sidewalls of the PGaN crystallites [26]. The superior optical properties of the 60-minute PGaN suggest that it could hold significant potential for sensor or optical applications [26].

4. CONCLUSION

The present study successfully fabricated PGaN samples using the LT-PEC technique under different etching durations. LT-PEC produced hexagonal-like porous structures with the pore size, density, and porosity varying depending on the etching duration. Both porosity and pore size were increased with longer etching duration, suggesting that LT-PEC duration plays a significant role in pore formation on the GaN surface. The increase in porosity coupled with smaller pore diameters, was influenced by the etching temperature. Therefore, temperature significantly affects the properties of PGaN. Additionally, longer etching duration resulted in deeper etching of the GaN, leading to an

Table 2. The peak positions at E_2(high), A_1(TO), and E_1(TO) of PGaN samples etched via LT-PEC at various etching durations

Samples	E_2(high)			A_1(TO)	E_1(TO)	Stress relaxation (GPa)
	Peak position (cm^{-1})	Intensity (arb. unit)	Peak shift (cm^{-1})	Peak position (cm^{-1})	Peak position (cm^{-1})	
as-grown	569.98	47065.60	-	-	-	-
45 minutes	569.15	60016.98	0.83	532.42	559.59	0.20
60 minutes	568.28	80662.10	1.70	532.42	559.59	0.40
90 minutes	568.19	76049.80	1.79	532.42	559.59	0.42

increase in surface roughness and estimated average pore depth. The Raman study revealed that stress relaxation was observed in the PGaN samples. The 60-minute PGaN sample exhibited the highest Raman intensity and superior optical behaviour compared to the as-grown GaN, making it highly suitable for application in efficient optoelectronic devices. Overall, this investigation demonstrates that LT-PEC under different etching durations significantly influences the structural and optical properties of PGaN samples.

ACKNOWLEDGMENTS

This project was funded by the Universiti Teknologi MARA through the Geran Penyelidikan MyRA (600-RMC/GPM ST 5/3 (023/2021)). The authors would like to thank Universiti Teknologi MARA Cawangan Pulau Pinang, the staff of the Nano-optoelectronics Research and Technology (NOR) laboratory and Science and Engineering Research Centre (SERC) of Universiti Sains Malaysia for supporting this research.

REFERENCES

[1] A. P. Vajpeyi *et al.*, "High Optical Quality Nanoporous GaN Prepared by Photoelectrochemical Etching," *Electrochemical and Solid-State Letters*, vol. 8, no. 4, p. G85, 2005, doi: 10.1149/1.1861037.

[2] M. Ainorkhilah *et al.*, "Enhanced Properties of Porous GaN Prepared by UV Assisted Electrochemical Etching," *Advanced Materials Research*, vol. 364, pp. 90–94, Oct. 2011, doi: 10.4028/www.scientific.net/AMR.364.90.

[3] J. H. Edgar, S. Strite, I. Akasaki, H. Amano, and C. Wetzel, *Properties, Processing and Applications of Gallium Nitride and Related Semiconductors*, illustrated ed. the University of Michigan: INSPEC, 1999.

[4] L. S Chuah, Z. Hassan, C. W Chin, and H. Abu Hassan, "Surface Morphology And Formation Of Nanostructured Porous GaN By UV-Assisted Electrochemical Etching," in *World Academy Of Science, Engineering And Technology 55*, 2009, pp. 16–19.

[5] R. Radzali, N. Zainal, F. K. Yam, and Z. Hassan, "Nanoporous InGaN of high In composition prepared by KOH electrochemical etching," *Materials Science in Semiconductor Processing*, vol. 16, no. 6, pp. 2051–2057, Dec. 2013, doi: 10.1016/j.mssp.2013.07.035.

[6] N. S. M. Razali *et al.*, "Investigation on the Effect of Direct Current and Integrated Pulsed Electrochemical Etching of n-Type (100) Silicon," *Acta Physica Polonica A*, vol. 135, no. 4, pp. 697–701, Apr. 2019, doi: 10.12693/APhysPolA.135.697.

[7] Y. Alifragis, A. Georgakilas, G. Konstantinidis, E. Iliopoulos, A. Kostopoulos, and N. A. Chaniotakis, "Response to anions of AlGaN/GaN high-electron-mobility transistors," *Applied Physics Letters*, vol. 87, no. 25, Dec. 2005, doi: 10.1063/1.2149992.

[8] A. Mahmood, Z. Hassan, Yam Fong Kwong, Chuah Lee Siang, and M. B. Md Yunus, "Photoluminescence, raman and X-ray diffraction studies of porous GaN grown on sapphire," in *2011 IEEE Colloquium on Humanities, Science and Engineering*, IEEE, Dec. 2011, pp. 677–681. doi: 10.1109/CHUSER.2011.6163819.

[9] T. L. Rittenhouse, P. W. Bohn, and I. Adesida, "Structural and spectroscopic characterization of porous silicon carbide formed by Pt-assisted electroless chemical etching," *Solid State Communications*, vol. 126, no. 5, pp. 245–250, May 2003, doi: 10.1016/S0038-1098(03)00130-3.

[10] R. Radzali, Z. Hassan, N. Zainal, and F. K. Yam, "Nanoporous InGaN prepared by KOH electrochemical etching with different light sources," *Microelectronic Engineering*, vol. 126, pp. 107–112, Aug. 2014, doi: 10.1016/j.mee.2014.06.027.

[11] L. A. Balagurov, B. A. Loginov, E. A. Petrova, A. Sapelkin, B. Unal, and D. G. Yarkin, "Formation of porous silicon at elevated temperatures," *Electrochimica Acta*, vol. 51, no. 14, pp. 2938–2941, Mar. 2006, doi: 10.1016/j.electacta.2005.09.022.

[12] R. Radzali, N. Zainal, F. K. Yam, and Z. Hassan, "Characteristics of porous GaN prepared by KOH photoelectrochemical etching," *Materials Research Innovations*, vol. 18, no. sup6, pp. S6-412-S6-416, Dec. 2014, doi: 10.1179/1432891714Z.000000000989.

[13] D. J. Blackwood and Y. Zhang, "The effect of etching temperature on the photoluminescence emitted from, and the morphology of, p-type porous silicon," *Electrochimica Acta*, vol. 48, no. 6, pp. 623–630, Feb. 2003, doi: 10.1016/S0013-4686(02)00731-4.

[14] J. W. Seo, C. S. Oh, H. S. Cheong, J. W. Yang, C. J. Youn, and K. Y. Lim, "UV-assisted electrochemical oxidation of GaN," *Journal of the Korean Physical Society*, vol. 41, no. 6, pp. 1017–1020.

[15] E. Trichas, M. Kayambaki, E. Iliopoulos, N. T. Pelekanos, and P. G. Savvidis, "Resonantly enhanced selective photochemical etching of GaN," *Applied Physics Letters*, vol. 94, no. 17, Apr. 2009, doi: 10.1063/1.3122932.

[16] J. Yu, L. Zhang, J. Shen, Z. Xiu, and S. Liu, "Wafer-scale porous GaN single crystal substrates and their application in energy storage," *CrystEngComm*, vol. 18, no. 27, pp. 5149–5154, 2016, doi: 10.1039/C6CE00741D.

[17] F. K. Yam, Z. Hassan, and S. S. Ng, "Porous GaN prepared by UV assisted electrochemical etching," *Thin Solid Films*, vol. 515, no. 7–8, pp. 3469–3474, Feb. 2007, doi: 10.1016/j.tsf.2006.10.104.

[18] F. Zulkifli, R. Radzali, A. F. Abd Rahim, A. Mahmood, N. S. Mohd Razali, and A. Abu Bakar, "Influence of different etching methods on the structural properties of porous silicon," *Microelectronics International*, vol. 39, no. 3, pp. 101–109, Jun. 2022, doi: 10.1108/MI-01-2022-0009.

[19] G. D. Sulka, "Highly Ordered Anodic Porous Alumina Formation by Self-Organized Anodizing," in *Nanostructured Materials in Electrochemistry*, Wiley, 2008, pp. 1–116. doi: 10.1002/9783527621507.ch1.

[20] N. H. Astuti, N. A. Wibowo, and M. R. S. S. N. Ayub, "The Porosity Calculation of Various Types of Paper Using Image Analysis," *Jurnal Pendidikan Fisika Indonesia*, vol. 14, no. 1, pp. 46–51, Jan. 2018, doi:

10.15294/jpfi.v14i1.9878.

[21] A. F. Abd Rahim *et al.*, "Crystal orientation dependence of alternating current photo-assisted (ACPEC) porous silicon for potential optoelectronic application," *Microelectronics International*, vol. 37, no. 1, pp. 46–53, Dec. 2019, doi: 10.1108/MI-08-2019-0052.

[22] S. N. Sohimee, Z. Hassan, N. M. Ahmed, R. Radzali, H. J. Quah, and W. F. Lim, "Comparative Studies between Porous Silicon and Porous P-Type Gallium Nitride Prepared Using Alternating Current Photo-Assisted Electrochemical Etching Technique," *Journal of Physics: Conference Series*, vol. 1535, no. 1, p. 012044, May 2020, doi: 10.1088/1742-6596/1535/1/012044.

[23] S. N. Sohimee, Z. Hassan, N. Mahmoud Ahmed, L. W. Foong, and Q. Hock Jin, "Effect of Different UV Light Intensity on Porous Silicon Fabricated by Using Alternating Current Photo-Assisted Electrochemical Etching (ACPEC) Technique," *Journal of Physics: Conference Series*, vol. 1083, p. 012034, Aug. 2018, doi: 10.1088/1742-6596/1083/1/012034.

[24] A. M. Almanza-Workman *et al.*, "Characterization of highly hydrophobic coatings deposited onto pre-oxidized silicon from water dispersible organosilanes," *Thin Solid Films*, vol. 423, no. 1, pp. 77–87, Jan. 2003, doi: 10.1016/S0040-6090(02)00997-5.

[25] A. P. Vajpeyi *et al.*, "Influence of Rapid Thermal Annealing on the Luminescence Properties of Nanoporous GaN Films," *Electrochemical and Solid-State Letters*, vol. 9, no. 4, p. G150, 2006, doi: 10.1149/1.2176889.

[26] J. Li, X. Xi, S. Lin, Z. Ma, X. Li, and L. Zhao, "Ultrahigh Sensitivity Graphene/Nanoporous GaN Ultraviolet Photodetectors," *ACS Applied Materials & Interfaces*, vol. 12, no. 10, pp. 11965–11971, Mar. 2020, doi: 10.1021/acsami.9b22651.

[27] M. Kuball, "Raman spectroscopy of GaN, AlGaN and AlN for process and growth monitoring/control," *Surface and Interface Analysis*, vol. 31, no. 10, pp. 987–999, Oct. 2001, doi: 10.1002/sia.1134.

[28] T. L. Williamson, D. J. Díaz, P. W. Bohn, and R. J. Molnar, "Structure–property relationships in porous GaN generated by Pt-assisted electroless etching studied by Raman spectroscopy," *Journal of Vacuum Science & Technology B: Microelectronics and Nanometer Structures Processing, Measurement, and Phenomena*, vol. 22, no. 3, pp. 925–931, May 2004, doi: 10.1116/1.1695335.

[29] F. K. Yam, Z. Hassan, L. S. Chuah, and Y. P. Ali, "Investigation of structural and optical properties of nanoporous GaN film," *Applied Surface Science*, vol. 253, no. 18, pp. 7429–7434, Jul. 2007, doi: 10.1016/j.apsusc.2007.03.032.

[30] K. Al-heuseen, M. R. Hashim, and N. K. Ali, "Enhanced optical properties of porous GaN by using UV-assisted electrochemical etching," *Physica B: Condensed Matter*, vol. 405, no. 15, pp. 3176–3179, Aug. 2010, doi: 10.1016/j.physb.2010.04.043.

[31] Ch. Ramesh *et al.*, "Laser molecular beam epitaxy growth of porous GaN nanocolumn and nanowall network on sapphire (0001) for high responsivity ultraviolet photodetectors," *Journal of Alloys and Compounds*, vol. 770, pp. 572–581, Jan. 2019, doi: 10.1016/j.jallcom.2018.08.149.

[32] Y. Xiao, W.-G. Zhang, Z.-T. Tan, G.-B. Pan, and Z. Peng, "High switch ratio, self-powered ultraviolet photodetector based on a ZnOEP/GaN p-n heterojunction with porous structure on GaN," *Chemical Physics Letters*, vol. 739, p. 136981, Jan. 2020, doi: 10.1016/j.cplett.2019.136981.